JOURNAL OF CATALYSIS 148, 478–492 (1994)

Transmission Electron Microscopy and Energy Dispersive X-Ray Spectroscopy Studies of Pt–Re/γ-Al_2O_3 Catalysts

Z. Huang, J. R. Fryer, C. Park, D. Stirling, and G. Webb

Department of Chemistry, University of Glasgow, Glasgow G12 8QQ, United Kingdom

Received August 27, 1993; revised February 3, 1994

A series of Pt/γ-Al_2O_3, Re/γ-Al_2O_3, and Pt-Re/γ-Al_2O_3 catalysts have been studied by transmission electron microscopy and energy dispersive X-ray spectroscopy. It has been shown that rhenium was not alloyed with platinum, but widely dispersed on the surface of alumina. Two types of platinum were found: (i) three-dimensional metallic particles, and (ii) small particles consisting of a few platinum atoms. Some aggregation of the platinum particles occurred during use of the catalysts in the reforming of octane. It is suggested that the interaction of rhenium with the alumina support and therefore the modification to the platinum play an essential role in promoting the enhanced stability and selectivity of these catalysts to cycloalkanes and aromatics in reforming reactions. © 1994 Academic Press, Inc.

INTRODUCTION

The addition of a second metal such as Re, Sn, Ir, or Ge to Pt/γ-Al_2O_3 catalysts improves the stability and selectivity of the catalysts in catalytic reforming reactions. However, despite Pt–Re/γ-Al_2O_3 having been used as a reforming catalyst for two decades, the origin of the improvement is still far from clear. Deposition of surface carbon is a major factor in determining catalyst lifetime in metal-catalysed reactions of hydrocarbons, and rhenium has been shown to extend the lifetime by modifying the type rather than the amount of carbon deposited (1). The main points of contention appear to be whether or not the second metal is alloyed with platinum and, if not alloyed, how the second metal is distributed over the Pt/γ-Al_2O_3 catalyst. The term "alloy" used in this context does not necessarily refer to the composition for bulk alloy formation, but, rather, it refers to two elements in the metallic state which are in intimate contact with each other. Such metal composites are sometimes referred to as bimetallic clusters and we do not differentiate the terms alloy and bimetallic cluster in this paper.

In recent years, the ability of the Pt–Re/γ-Al_2O_3 system to undergo alloy formation has been extensively studied. It seems that the observed state of rhenium, and whether rhenium is alloyed with platinum, is highly dependent on the probe method employed, the pretreatment and starting materials (2–5), and the support. Issacs and Petersen (6–8) used oxygen chemisorption and titration, and temperature programmed reduction (TPR) to characterise the metal dispersion and alloy formation. It was found that the hydrogen chemisorption of Pt was suppressed and its oxygen chemisorption increased by the presence of rhenium. This led the authors to the conclusion that there was some interaction between the metals and possibly alloy formation. Furthermore, TPR studies showed that rhenium oxide was more easily reduced in the presence of platinum, indicating that a Pt/Re alloy may be formed (9–11). Microreactor reforming experiments showed that the addition of rhenium to Pt/γ-Al_2O_3 catalysts increased the catalytic activity and selectivity in reforming reactions. Alloy formation was suggested as an interpretation of this catalytic improvement (12–15).

Other studies led to different conclusions. Johnson and LeRoy (16) leached reduced bimetallic catalysts by using HBF_4, and investigated the solid residue by X-ray diffraction and the leached solution by X-ray fluorescence. They found that the rhenium was in the ReO_2 state and strongly associated with the surface of alumina, whilst platinum was in the metallic state. Studies by Kelley *et al.* (5) using transmission electron microscopy (TEM), energy dispersive X-ray spectroscopy (EDX), and ion scattering spectroscopy concluded that rhenium was not significantly associated with platinum and was widely dispersed on the support surface. Short *et al.* (17) provided evidence by synchrotron radiation X-ray absorption spectroscopy that rhenium was neither in the zero oxidation state nor significantly associated with platinum. Infrared studies by Peri (18) showed no evidence of alloy formation in commercial Pt–Re/γ-Al_2O_3 catalysts. In contrast to the TPR studies reported earlier, further work using this technique has indicated that alloy formation does not occur (19–21). A reduction mechanism has been proposed (21) in which hydrogen was activated by reduced platinum and transferred to ReO_x aggregates across a hydrated alumina

0021-9517/94 $6.00

surface (H_2 spillover). This mechanism is also supported by the work of Bertolacini and Pellet, who found that a physical mixture of Pt/γ-Al_2O_3 and Re/γ-Al_2O_3 showed the same improved catalytic properties as the conventional bimetallic catalyst (22).

This diversity of opinion regarding the nature of the Pt–Re interaction in supported Pt–Re/γ-Al_2O_3 catalysts emphasises the need for careful reproducible control of the preparation of these reforming catalysts. Furthermore, their low metal loading and high dispersion make analysis of the structure and composition of the resultant small metal particles difficult. The transmission electron microscope (TEM) has proved to be a powerful instrument to study this kind of system (23–25), and elemental analysis, in EDX, has provided a direct probe to investigate the composition of small particles. We report here a study of Pt/γ-Al_2O_3, Re/γ-Al_2O_3, and Pt–Re/γ-Al_2O_3 catalysts which were commercially purchased or prepared from supported precursor salts by standardised activation procedures using a parallel combination of TEM and EDX.

EXPERIMENTAL

1. Catalysts

Both commercially purchased and laboratory prepared catalysts were used. The commercial catalysts were EUROPT-3 (0.3 wt.% Pt/γ-Al_2O_3, 0.95 wt.% Cl) and EUROPT-4 (0.3 wt.% Pt–0.3 wt.% Re/γ-Al_2O_3, 0.95 wt.% Cl). Laboratory-prepared catalysts included 0.3 wt.% Re/γ-Al_2O_3, 3.0 wt.% Re/γ-Al_2O_3, 3.0 wt.% Pt/γ-Al_2O_3, and 3.0 wt.% Pt–3.0 wt.% Re/γ-Al_2O_3.They were prepared by impregnation of γ-Al_2O_3 with the appropriate concentration of NH_4ReO_4 aqueous solution and/or H_2PtCl_6 aqueous solution to give the required metal loadings. The support used was commercial pelletised γ-Al_2O_3 (CK300, BET area 200 m^2/g) consisting of cylindrical pellets about 2 mm in diameter and ranging from 2 mm to 10 mm in length. After impregnation, the pellets were dried in flowing air at 383 K for 4 h. This will be referred to as the catalyst precursor. The bimetallic catalyst precursor was obtained by firstly impregnating the γ-Al_2O_3 with the required concentration of NH_4ReO_4 aqueous solution and drying it at 383 K in flowing air, then carrying out a second impregnation with the required amount of H_2PtCl_6 aqueous solution, and finally drying again at 383 K in flowing air.

All the above catalyst precursors were subjected to the following activation process:

(a) Calcination: The catalyst precursors were heated from room temperature to 673 K at 5 K/min in flowing air (60 cm^3/min), held at this temperature for 4 h and then cooled to room temperature.

(b) Flushing: He (60 cm^3/minute) was passed over the calcined catalyst precursors for 1 h at room temperature.

(c) Reduction: The reduction was carried out in flowing H_2 (60 cm^3/min), with a programmed temperature increase of 5 K/min from room temperature to 673 K, and maintained at this temperature for 2 h. The catalysts were then cooled to room temperature in flowing hydrogen.

The same reoxidation, flushing, and reduction procedures were repeated for the above-treated specimens to investigate any further changes in the catalysts. Finally, passivation was carried out with 1.0 vol.% air/He for specimens for normal TEM investigation.

2. Catalyst Testing

Octane reforming was carried out in a microreactor which will be described elsewhere (26) in which the reaction conditions were as follows: H_2/octane ratio = 6/1; reaction temperature = 783 K; reaction pressure = 110 psig; weight hourly space velocity (WHSV) = 2 h^{-1}. Analysis of the reaction products was carried out by sampling to a Shimadzu gas chromatograph.

3. Carbon Monoxide Chemisorption

CO chemisorption was performed in a system similar to that described in an earlier publication (27). Typically, 0.5 g catalyst was used for the chemisorption studies at the 0.3 wt.% metal loading and 0.1–0.2 g for higher loadings. Each catalyst was heated from room temperature to 673 or 953 K in some cases (Table 1) in flowing hydrogen and held at this temperature for 2 h. The catalyst was then cooled to room temperature in flowing helium and the adsorption experiment was carried out by injecting pulses of known amounts of CO (4.7 cm^3, 17 Torr) into the helium carrier-gas stream and hence onto the catalyst. These injections were repeated until no further CO was adsorbed. The amount of CO adsorbed in each pulse was determined by subtracting the observed number of moles of CO that had not been retained by the catalyst from the inlet CO concentration. The total amount of CO adsorbed was a summation of these values.

4. Electron Microscopy and EDX

The microscope was an ABT-EM002B instrument in which an EDX system LINK2000-QX with a windowless detector was installed. The microscope was usually operated at 200 kV, but sometimes 160 kV was used to obtain higher contrast image of small particles. An improved LaB_6 filament was used. The energy resolution of the EDX system was 138 eV at 5.9 keV.

TEM specimens were prepared by placing a drop of ethanol solution, containing the ground catalyst powder in suspension, on a carbon-film-coated copper grid. Some specimens were kept in the microscope overnight before

TABLE 1

TEM and EDX Results for Pt/γ-Al_2O_3, Re/γ-Al_2O_3, and Pt–Re/γ-Al_2O_3 Catalysts

Specimen	EUROPT-3	EUROPT-4	0.3 wt.% Re	3 wt.% Re	3 wt.% Pt–3 wt.% Re
Fresh	x	x	x	x	x
Calcined	x	x	x	x	1–10 nm, Pt, few ReO_x
Reduced	x	2–3 nm Pt	x	x	1–10 nm, small Pt, few ReO_2
Oxidised	x	2–3 nm Pt	x	x	1–10 nm Pt
Reduced	x	2–4 nm Pt	x	x	1–10 nm Pt, more small particles
Reduced to 1023 K			x	2–10 nm ReO_x	
Used 24 h at 773 K	1–20 nm Pt	1–20 nm Pt			

study to minimise possible contamination during EDX spectrum collection. A beam of 10 nm in diameter, which covered a particle, was used to generate an EDX spectrum. The collection time was usually 100 s. During the collection, the beam was sometimes spread (underfocussed or overfocussed) for a while to obtain an image of the particle and the beam relocated on the particle to compensate for any specimen shift. The sensitivity of the EDX (28) system was about 400–800 platinum or rhenium atoms, or about 2–3 nm in particle size.

For quantitative EDX analysis it was necessary to determine the detector efficiency factor for oxygen. The detector efficiency factors for aluminum and platinum were unity. The γ-Al_2O_3 was used as a standard for calibration.

Generally, $C_\alpha/C_\beta = (K\alpha/K_\beta)\ (I_\alpha/I_\beta)$, where C_α is the weight percent of the α element, K_α is the elemental sensitivity factor of α, and I_α is the EDX intensity of α.

When the detector efficiency of the (K, L, M) line of element α is ε instead of unity, the real intensity will be $I_{\alpha(\text{real})}$ and $I_{\alpha(\text{real})} = \varepsilon \cdot I_\alpha$.

Ten values for the detector efficiency factor of oxygen were obtained from their respective spectra. These values were close to each other ($< \pm 5\%$) and averaged to be 3.5. The real intensity of oxygen should then be equal to the observed intensity multiplied by 3.5.

The elemental sensitivity factors K_α are taken from the Operator's Manual of the LINK system. They are $K_{OK} = 1.0$, $K_{AlK} = 1.17$, $K_{ReM} = 1.56$.

5. *Ex Situ TEM and EDX*

Although catalysts were generally passivated after reduction before examination in the microscope, some *ex situ* studies were also carried out in which the catalysts were transferred after activation or reforming directly from microreactors to a dry-box filled with nitrogen without being exposed to air. The oxygen concentration in the dry-box was about 10 ppm. TEM samples were prepared in the dry-box and then mounted onto an environmental specimen holder. The environmental specimen holder enabled the TEM sample to be transferred into the microscope without being exposed to air.

RESULTS AND DISCUSSION

1. *Catalyst Reforming*

After several hours on line, i.e., under "steady state" conditions, the overall conversion of *n*-octane was higher for EUROPT-4 than EUROPT-3 (57.0% and 48.4%, respectively). EUROPT-4 also showed higher stability, the conversion of *n*-octane falling to 28.3% on EUROPT-3 but only 40.6% on EUROPT-4 after 45 h on line. This result is not really surprising since rhenium is well known to modify the type of carbon deposited (1). The selectivities to aromatics of each of these catalysts are plotted in Fig. 1. Although the initial selectivities were similar, the

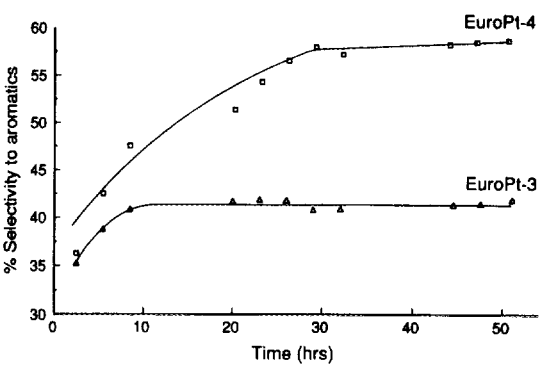

FIG. 1. The selectivities to aromatics for EUROPT-3 and EUROPT-4 in octane reforming.

selectivity to aromatics increased from 36.3% to 58.7% with increasing time on stream for EUROPT-4 but only from 35.2% to 41.8% in the case of EUROPT-3. The poorer performance of EUROPT-3 is likely to originate from the extensive formation of carbonaceous residues in this catalyst which results in catalyst deactivation. Overall, the isomerisation results were similar for both EUROPT-3 and EUROPT-4. Hydrogenolysis decreased significantly with time on stream for EUROPT-4 but only slightly for EUROPT-3. A more detailed analysis of these results will be published separately (26).

2. *TEM and EDX*

(*a*) *General observations.* A typical image of the EUROPT-4 catalyst precursor is shown in Fig. 2. No metal particles were detected in the catalyst prior to reduction, so the micrograph is representative of the γ-Al_2O_3. The appearance of the alumina crystallite was the same for all of the catalysts. The alumina crystals are randomly orientated in different directions, and show a range of contrast between the differently orientated crystals. Sometimes it was difficult to distinguish this contrast from the contrast of metal particles supported on alumina (29, 30), so elemental analysis was used to determine whether a contrast was generated by the higher atomic number of the metal, rather than orientation effects in the alumina. The TEM and EDX results are summarised in Table 1, where "x" indicates that no particles were found in the sample. The approximate particle size and particle composition are also presented.

(*b*) *Catalysts after calcination and reduction.* No metal particles were detected in EUROPT-3 even after reoxidation and reduction at 673 K. However, small particles about 2–3 nm in diameter were observed in EUROPT-4 after calcination and reduction (Fig. 3a) and EDX results confirmed that the particles were platinum. The dark circle around the platinum particle shown in Fig. 3a was due to contamination accumulated during the EDX spectrum collection. The Cu signal comes from the copper TEM grid. The Al and O come from the alumina support, and the C comes from the carbon support film. There was no evidence of Pt–Re alloy formation.

Platinum particles remained after a further reoxidation step. Some particle aggregation occurred during the second reduction for the EUROPT-4, some of the particles increasing in size from 3 to 4 nm (Fig. 4). The 0.227-nm lattice fringes visible in the micrograph correspond to the [111] planes of the crystalline platinum. A survey of a number of areas of the EUROPT-4 catalyst showed that the particle number density (number of the TEM visible particles per unit area) in the catalyst was quite small, suggesting that the platinum particles observed accounted

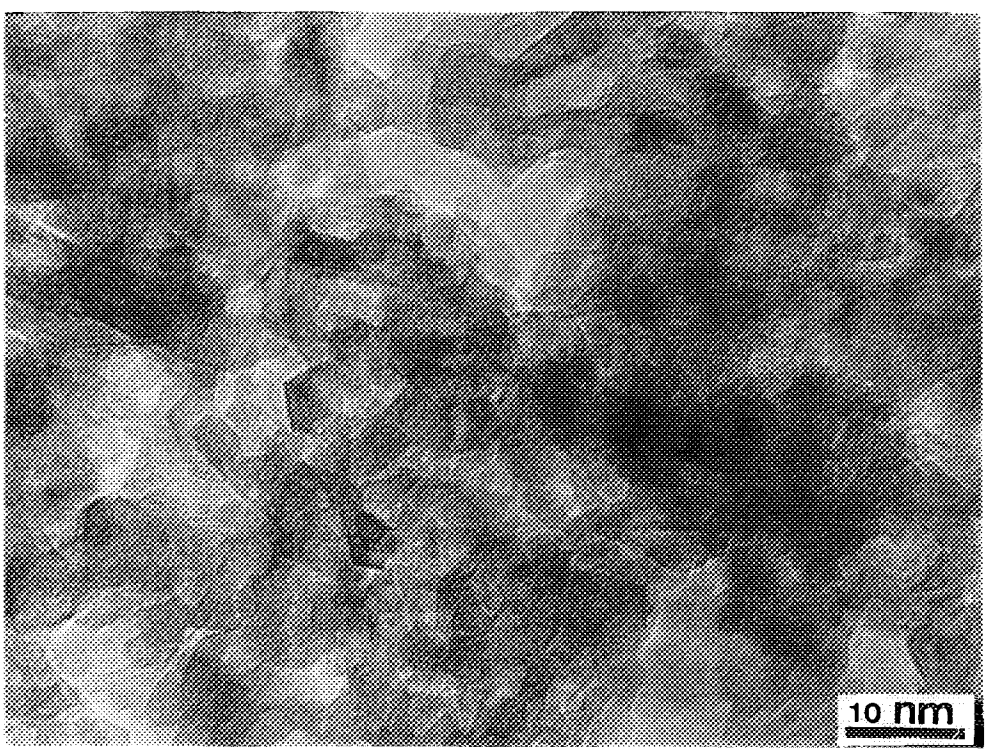

FIG. 2. Typical TEM micrograph of the EUROPT-4 precursor when no metal particles are observed.

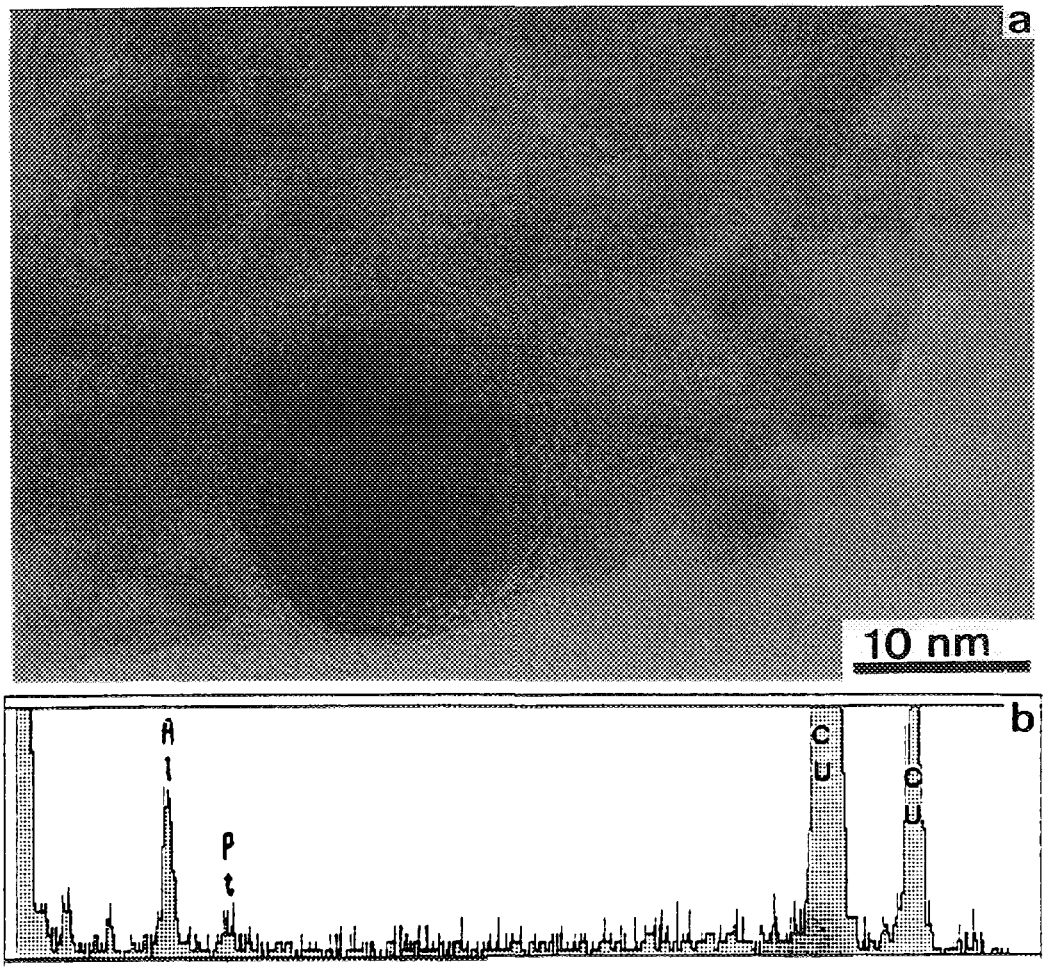

FIG. 3. EUROPT-4 after calcination in air at 673 K: (a) TEM micrograph; (b) EDX spectrum from the dark circular area in (a).

for only a small amount of total platinum in the catalyst, the majority of platinum being TEM-uinrecognizable small particles. It is therefore concluded that platinum in both EUROPT-3 and EUROPT-4 was highly dispersed. For a 3.0-wt.% $Pt/\gamma\text{-}Al_2O_3$ catalyst, a qualitative study showed that the particle number density was higher, and some small platinum particles (arrows in Fig. 5) about 1 nm in size were imaged. Although it is not possible to "see" particles smaller than 1 nm supported on thick $\gamma\text{-}Al_2O_3$, it is not unreasonable to suppose that there were some even smaller platinum particles (<1 nm) supported on the surface of alumina. Indeed, EDX signals due to platinum were obtained over a thicker area of specimen where no particles could be seen.

Monometallic rhenium catalysts did not readily undergo any particle aggregation. No particles were detected in either 0.3 wt.% $Re/\gamma\text{-}Al_2O_3$ or 3.0 wt.% $Re/\gamma\text{-}Al_2O_3$ catalysts after calcination and/or reduction at 673 K. Rhenium or rhenium oxide particles were only observed in the 3.0 wt.% $Re/\gamma\text{-}Al_2O_3$ (Fig. 6) catalyst after reduction at 1023 K. This indicated that the rhenium interacted more strongly with the alumina than the platinum, possibly forming either a dispersed two-dimensional $Re/\gamma\text{-}Al_2O_3$ phase or incorporating the rhenium in the $\gamma\text{-}Al_2O_3$ spinel structure. The existence of dispersed two-dimensional $Re/\gamma\text{-}Al_2O_3$ phases has been suggested before (31, 32) and this may account for the majority of the Re at low rhenium loadings (31).

Figure 7 shows an image of 3.0 wt.% Pt–3.0 wt.% $Re/\gamma\text{-}Al_2O_3$ after reduction. Qualitatively, the particle number density appeared much higher for 3.0 wt.% Pt–3.0 wt.% $Re/\gamma\text{-}Al_2O_3$ than that found in EUROPT-4, and particle sizes generally ranged from 1 to 10 nm. A few very large particles larger than 50 nm were also observed (Fig. 8). When the electron beam was focussed onto the edge of the particle (arrows) where the alumina was very thin, an EDX spectrum was obtained with a very strong Pt signal and a weak oxygen signal. This indicated that this particle

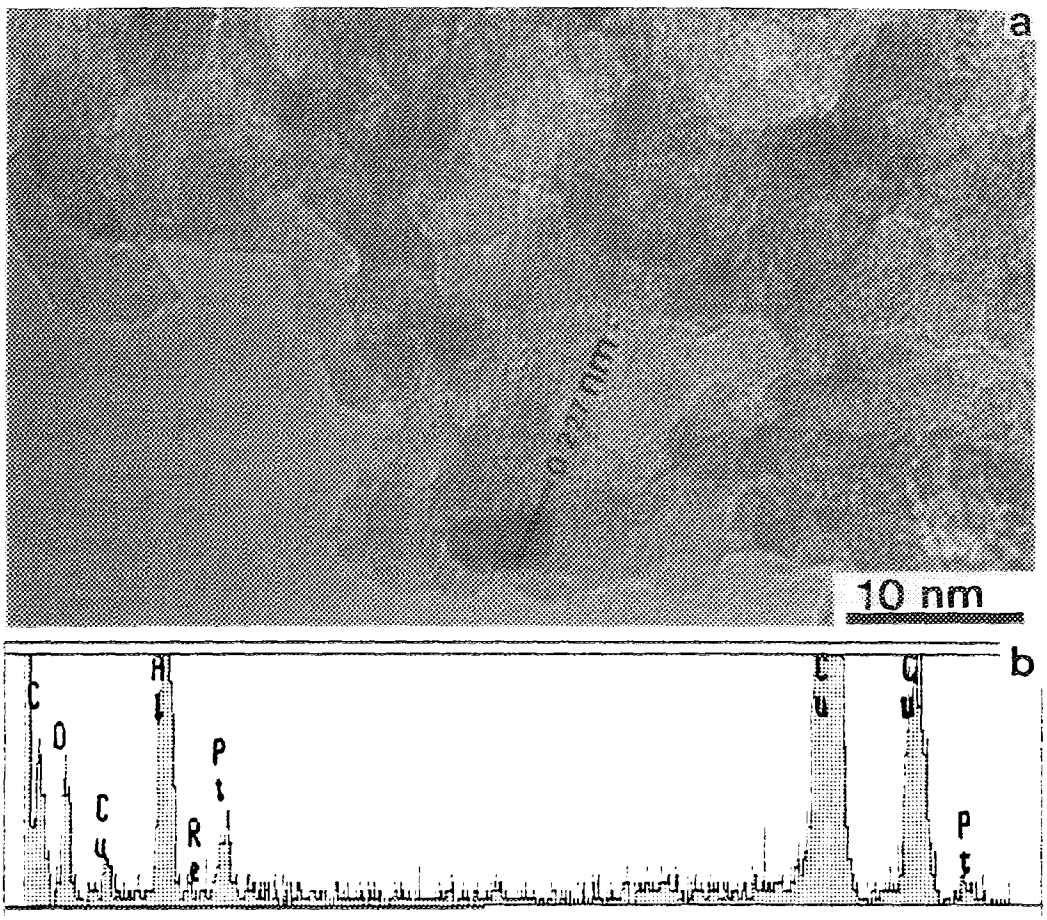

FIG. 4. EUROPT-4 after calcination and reduction at 673 K: (a) TEM micrograph; (b) EDX spectrum showing that the particle is platinum.

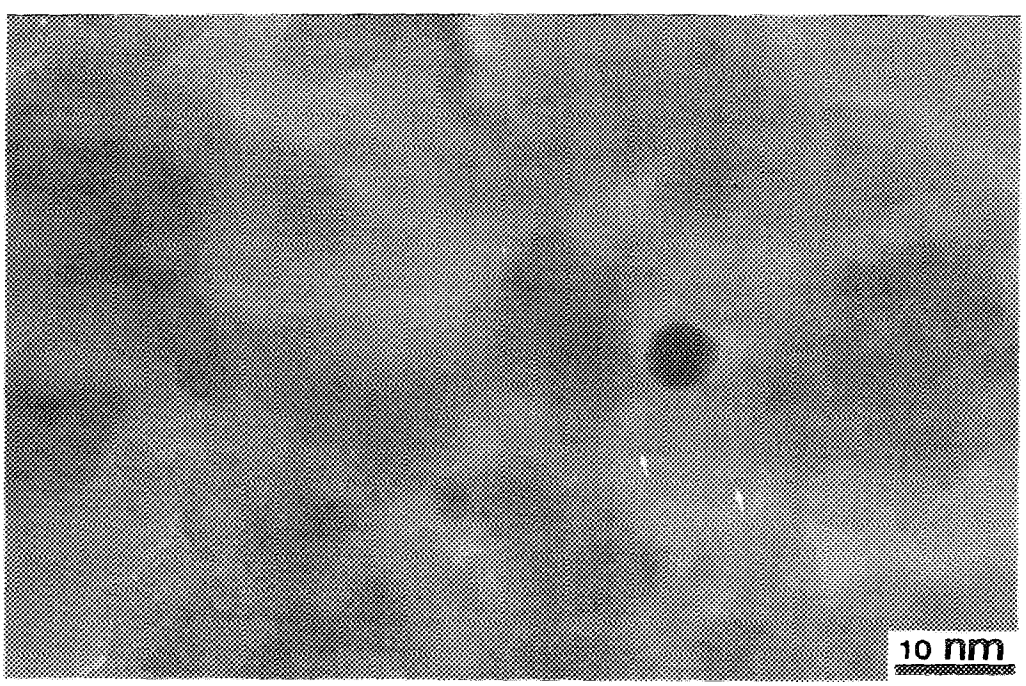

FIG. 5. TEM micrograph of 3.0 wt.% Pt/γ-Al_2O_3 catalysts. There are small Pt particles (~1 nm, arrows) as well as a large platinum particle.

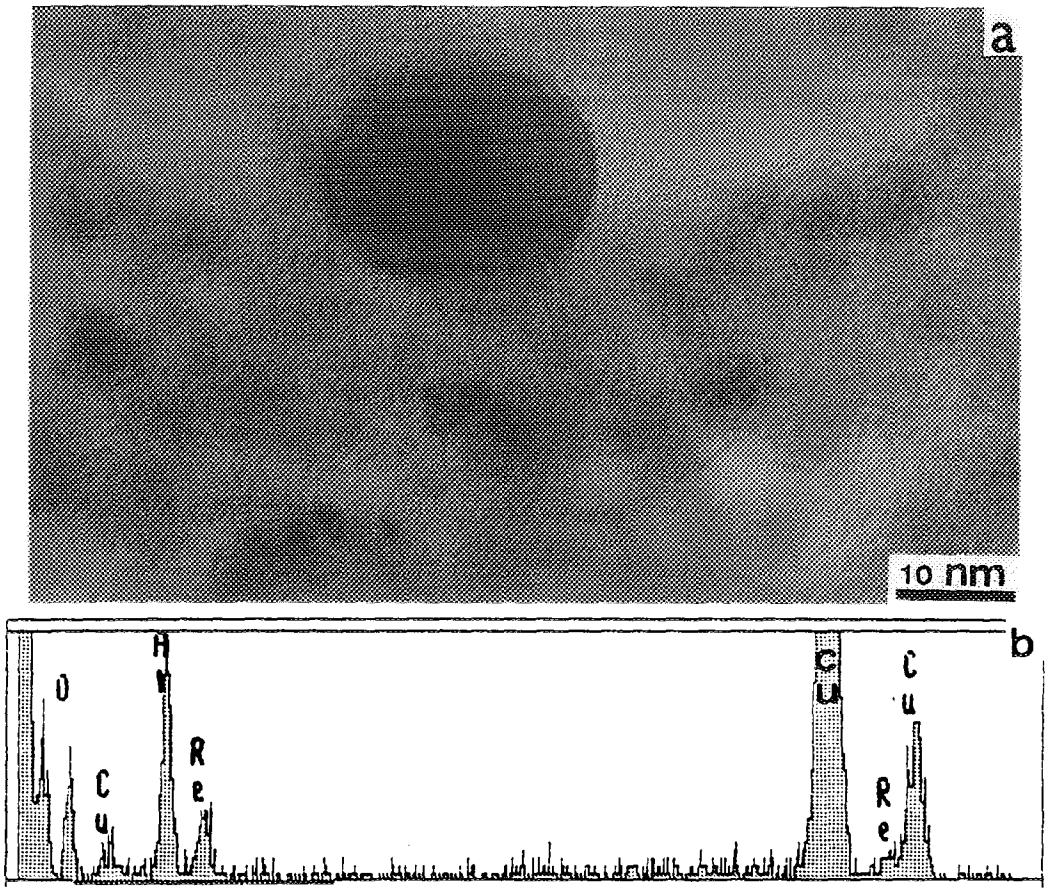

FIG. 6. 3.0 wt.% $Re/\gamma\text{-}Al_2O_3$ catalysts after reduction in flowing hydrogen at 1023 K: (a) TEM micrograph; (b) EDX spectrum from the dark area around the particle.

FIG. 7. TEM micrograph of 3.0 wt.% Pt–3.0 wt.% $Re/\gamma\text{-}Al_2O_3$ catalyst. The particle number density is higher than that in EUROPT-3 and EUROPT-4.

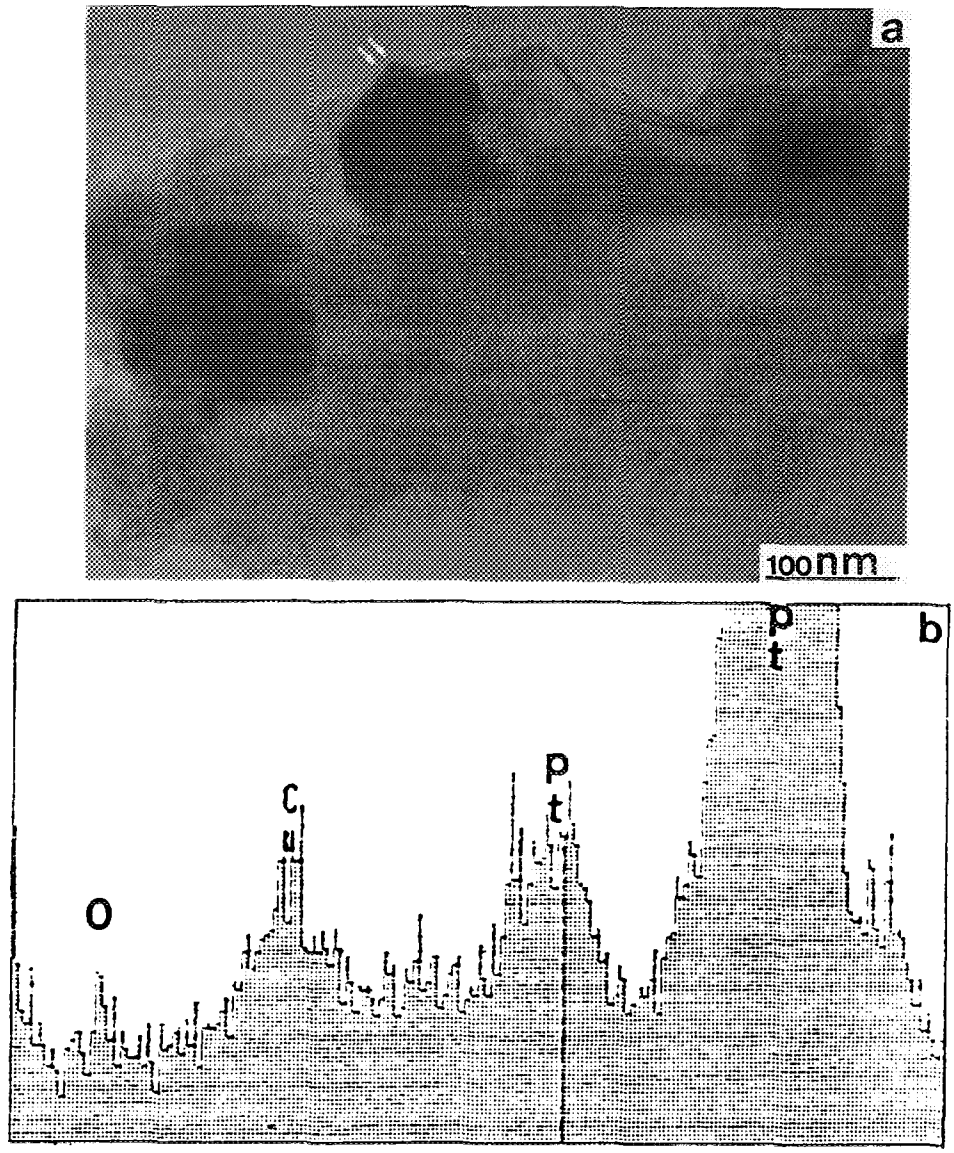

FIG. 8. 3.0 wt.% Pt–3.0 wt.% Re/γ-Al_2O_3 catalysts after reduction in hydrogen at 673 K: (a) TEM micrograph of a few very large particles; (b) EDX spectrum from the edge of a particle (arrows in (a)). The very strong Pt peak and very weak oxygen peak indicate that the platinum is in the metallic state.

was in the metallic state. The lattice image and microdiffraction patterns of a large number of particles were measured and found to be consistent with that for platinum metal. A few rhenium oxide particles were also detected. Figure 9 shows a particle supported on carbon film. Quantitative EDX analysis showed that the particle was rhenium oxide.

The experimental intensities were as follows:

$$I_{OK} = 365, \quad I_{AlK} = 311, \quad I_{ReM} = 3528.$$

The detector efficiency factor for oxygen was determined to be 3.5 (see Experimental section).

The real intensities should therefore be

$$I_{OK(real)} = 1278, \quad I_{AlK} = 311, \quad I_{ReM} = 3528.$$

The oxygen peak arose from oxygen in both Al_2O_3 and rhenium oxide. Thus, $I_{OK(real)} = I_{OK}(Al) + I_{OK}(Re)$,

$$I_{OK}(Al) = I_{AlK} \cdot K_{AlK} \cdot \frac{\text{mol. wt. of oxygen} \cdot 3}{\text{mol. wt. of aluminum} \cdot 2}, \text{ i.e.,}$$

$$I_{OK}(Al) = (1.17 \cdot 48)/(54 \cdot I_{AlK}) = 323, \quad \text{and}$$

$$I_{OK}(Re) = I_{OK(real)} - I_{OK}(Al) = 1278 - 323 = 955, \quad \text{then}$$

$$C_O/C_{Re} = (1.00/1.566) \cdot (955/3528) = 0.173.$$

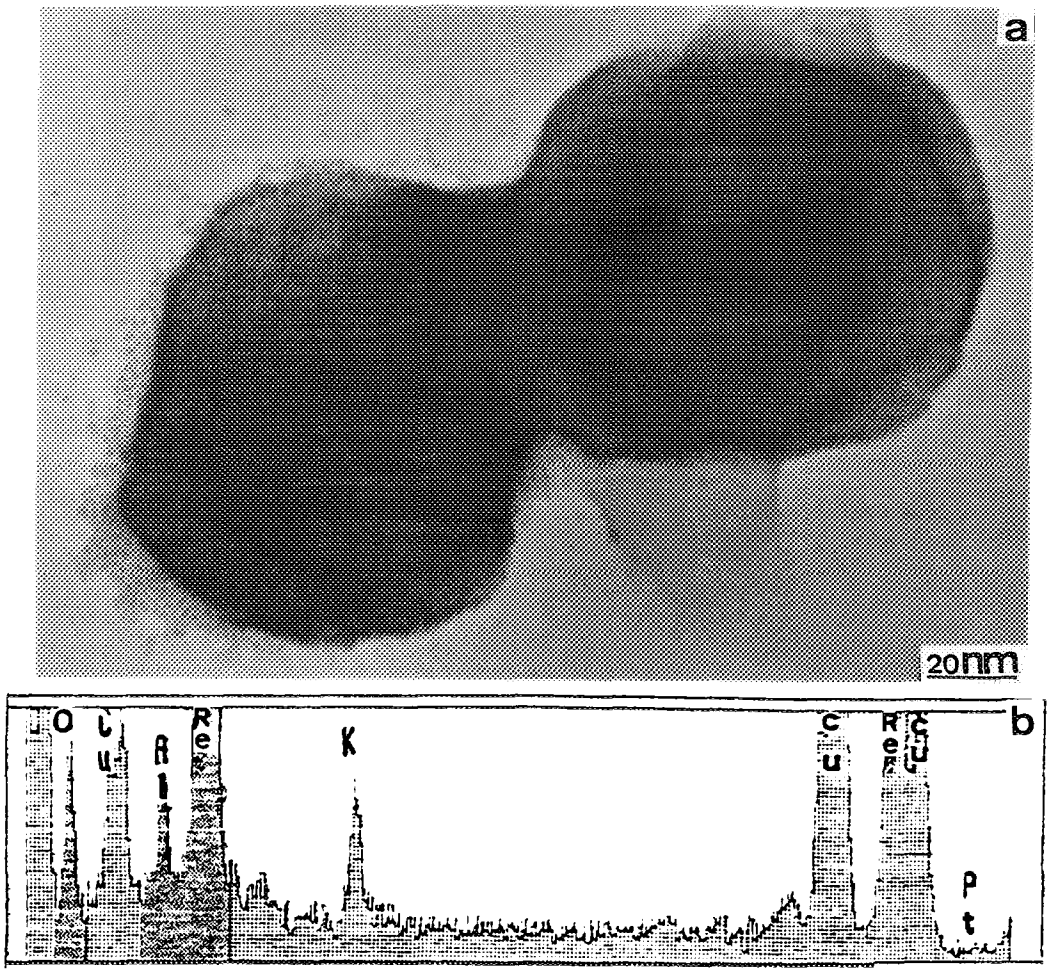

FIG. 9. 3.0 wt.% Pt–3.0 wt.% Re/γ-Al_2O_3 catalysts after reduction in H_2 at 673 K: (a) TEM micrograph of a very large particle; (b) EDX spectrum of the particle. A quantitative analysis of the EDX results shows that the particle is ReO_2.

This ratio enables the stoichiometry of the rhenium oxide ReO_x to be determined since X = (mol. wt. of rhenium)/(mol. wt. of oxygen)$\cdot C_O/C_{Re}$, i.e., $X = (186/16)\cdot 0.173 = 2.01$.

Therefore the rhenium oxide has the stoichiometry ReO_2.

A few more rhenium oxide particles on the support γ-Al_2O_3 were observed and the quantitative EDX analysis showed the stoichiometry ReO_x to be $X = 2.0 \pm 0.4$. This indicates that rhenium in large particles was in the ionic state, most probably as Re^{4+} in the bimetallic catalysts.

No metallic rhenium particles have been observed in the catalysts.

(c) *Catalysts after use in reforming.* Particle aggregation was evident for both EUROPT-3 (Fig. 10) and EUROPT-4 (Fig. 11) catalysts after use in reforming conditions, with platinum particles up to 20 nm in size being detected. EDX and microdiffraction studies showed that the particles were platinum. A significant number of small particles (<5 nm) were observed in addition to the 20-nm particles. Although the particles were mobile on the alumina surface under reaction conditions, as shown by their aggregation, no Pt–Re alloy was observed in EUROPT-4.

No Pt–Re alloy particles were observed when more than 200 particles were analysed in the EUROPT-4 and the 3.0 wt.% Pt–3.0 wt.% Re/γ-Al_2O_3 bimetallic catalysts (including both used and unused catalysts). Although this conclusion was ambiguous for small particles (2–4 nm) when the number of atoms within the particle is about the same as the EDX sensitivity (400–800 atoms), the accuracy should be within 4% for large particles of 10 nm in diameter. We could not rule out the possibility that a few percent of rhenium was dissolved in the platninum particle. However, it is unlikely that there was a significant amount of metallic rhenium alloyed with platinum in the small particles, because both platinum and metallic

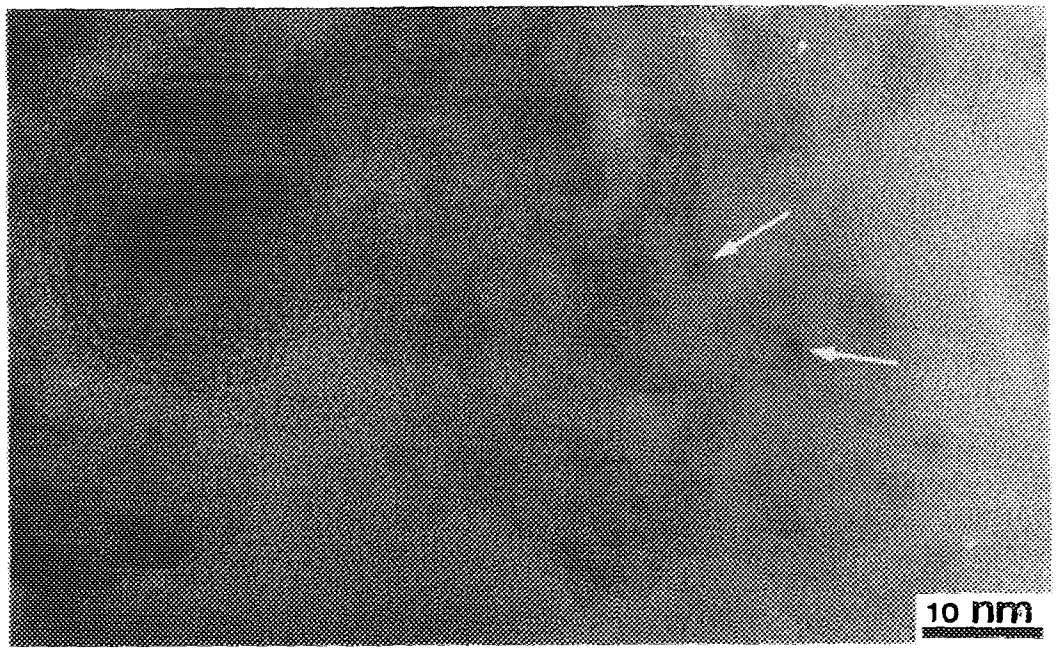

FIG. 10. TEM micrograph of EUROPT-3 after use in octane reforming. Small particles no larger than 1 nm in size (arrows) as well as a large platinum particle were observed in this image.

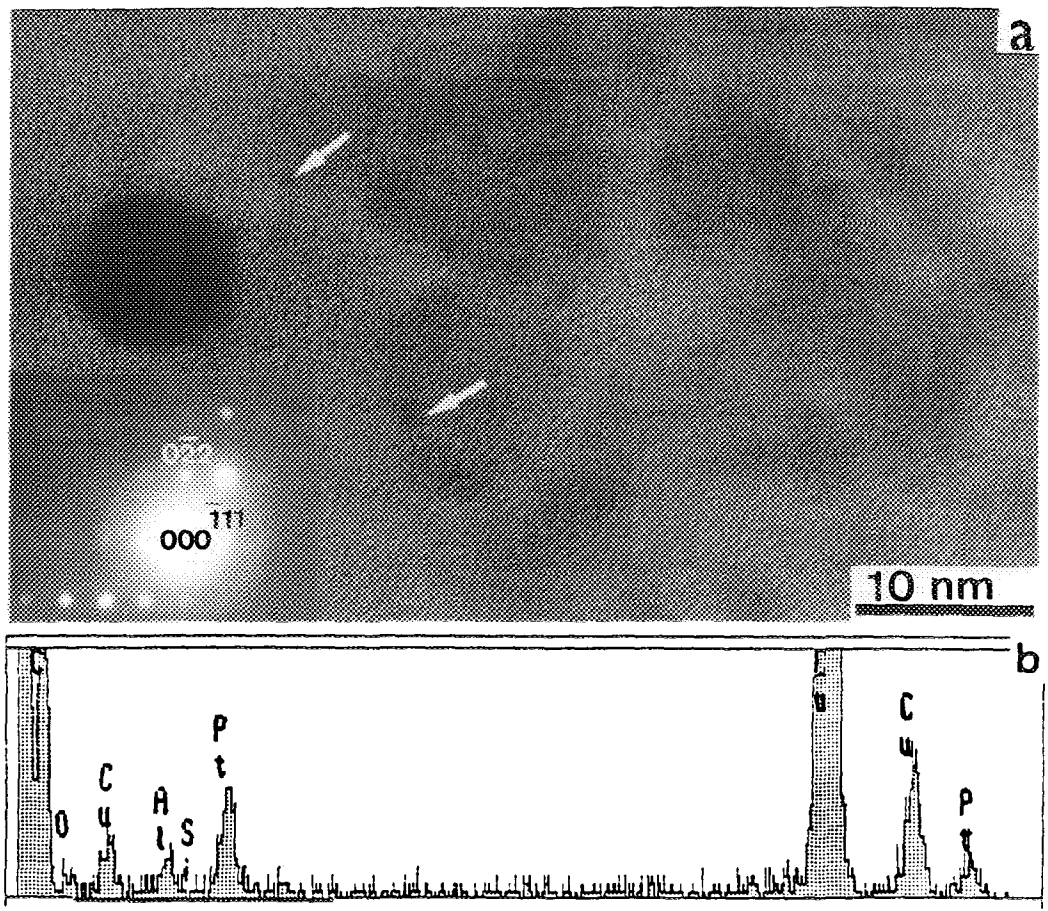

FIG. 11. EUROPT-4 after use in octane reforming: (a) TEM micrograph. Small particles (arrows) smaller than 1 nm in size coexist with a large particle in the micrograph. The inserted microdiffraction pattern of the large particle can be indexed to be the (211) pattern of the crystalline platinum. (b) EDX spectrum of the large particle.

rhenium were known to act as nuclei for catalysing the reduction of rhenium oxide (9–11, 21). If there was any alloy formation between platinum and rhenium, one would expect that the rhenium concentration in large particles (>10 nm) would exceed the EDX sensitivity. This has proved not to be the case. It is therefore concluded that no alloy formation occurred in the catalysts.

(*d*) *Metal distributions.* Although no Pt–Re clusters were formed in EUROPT-4 after use in reforming conditions, rhenium signals could be obtained from some thick specimen areas indicating that the rhenium was distributed around the platinum. This rhenium distribution was investigated further by varying the size of the electron beam used in the EDX experiment. In order to conduct this experiment, an area of the sample was selected which contained a single large platinum particle and a reasonably uniform thickness of alumina support around the particle (Fig. 12a). Initially, a beam about the same size (~10 nm) as the particle was used to generate an EDX spectrum, and the beam was then defocussed (underfocussed or overfocussed) to the larger size of 20 nm to obtain another spectrum. The collection time was generally around 100 s. The dead time and counts per second were kept the same for every spectrum. When the beam is spread, the total current of the beam will remain the same, so its intensity will decrease with the square of the beam size. At the same time, the specimen material included within the beam will increase as the square of the beam diameter. This means that the EDX intensity should be a constant if the element is uniformly distributed. Further spectra were collected using 50-, 100-, and 500-nm diameter beams, respectively. The intensities of platinum and rhenium were then plotted as a function of beam size (Fig. 12b). For comparison, the theoretical platinum intensity curve is included in Fig. 12b. This was derived by assuming that only the platinum particle was present on the alumina. The platinum intensity was then plotted against beam diameter.

Figure 12b shows that the observed platinum intensity was almost constant when the beam diameter was greater than or equal to 100 nm. The theoretical intensity curve based on a single platinum particle at the centre of the beam shows that the intensity should actually be zero when the beam is 100 nm or more. This indicates that a second type of platinum species was also present. This may consist of very small platinum particles which could not be resolved by TEM when the particles were supported on alumina. This hypothesis is supported by our previous assumption that small (<1 nm) platinum particles were present in the 3.0 wt.% Pt/γ-Al_2O_3 catalyst. This is also in agreement with previous work in this laboratory (33) in which quantitative X-ray diffraction and high resolution electron microscopy studies showed that the average platinum particle size was 0.9 nm in 0.5 wt.% Pt/γ-Al_2O_3 catalysts. For rhenium, the intensity was almost constant but decreased in the vicinity of the platinum particle. This variable beam size experiment was repeated for the 3.0 wt.% Pt–3.0 wt.% Re/γ-Al_2O_3 catalyst (Fig. 13). It was hoped that the higher platinum and rhenium EDX intensities resulting from the higher metal loadings would increase the sensitivity of the method for determining any Pt–Re interaction. The results were similar to those described above for EUROPT-4 indicating that there is no Pt–Re alloy formed under our experimental conditions even at the higher loadings. A possible explanation for these results is that the function of rhenium was to modify the alumina surface, and so alter the electronic properties of the small platinum particles. A similar mechanism has been proposed by Burch (34, 35), for Pt–Sn/γ-Al_2O_3 catalysts, where the tin component enhanced selectivity for isomerisation and aromatisation reactions in the reforming of *n*-hexane. The tin was stabilised as Sn(II) by interaction with the alumina support and could not therefore form Pt–Sn alloy.

(*e*) *Ex situ studies.* *Ex situ* studies were carried out using both calcined and reduced catalysts and catalysts after use in reforming. The TEM results for these oxygen-free prepared samples were identical to those obtained using the standard procedure of passivation of the reduced/reactor discharged samples in 1 vol.% air/helium. Furthermore, subsequent exposure of the *ex situ* samples to air for up to 24 h, did not change the particle morphology or size, indicating that the platinum (in the metallic state) and rhenium (as the oxide) were stable at room temperature in air, and that the observed results are representative of the particle morphology and size distribution of the catalysts in the reactor.

3. *Carbon Monoxide Adsorption*

The CO chemisorption results are summarised in Table 2. It was observed that the 3.0 wt.% Re/γ-Al_2O_3 catalyst adsorbed no CO after reduction at 673 and/or 953 K. This result suggests that the rhenium was not in the metallic state in the catalyst after reduction since metallic rhenium is known to adsorb CO (36, 37). The ratio of CO_{ad}/Pt for each catalyst can be found in the last column of Table 1. The maximum number of CO molecules that can be adsorbed per surface Pt atom has been determined to be 0.87 ± 0.07 (38, 39) for supported Pt particles with average sizes smaller than 5 nm. (The $CO/Pt_{surface}$ ratio decreases to about 0.5 for larger supported particles.) This gives a dispersion of around 74% for EUROPT-3. The CO_{ad}/Pt ratio for EUROPT-4 was found to be the same as that of EUROPT-3, in agreement with a previous CO chemisorption investigation (40) in this laboratory. Two explanations are possible for this result. (i) All the adsorbed CO

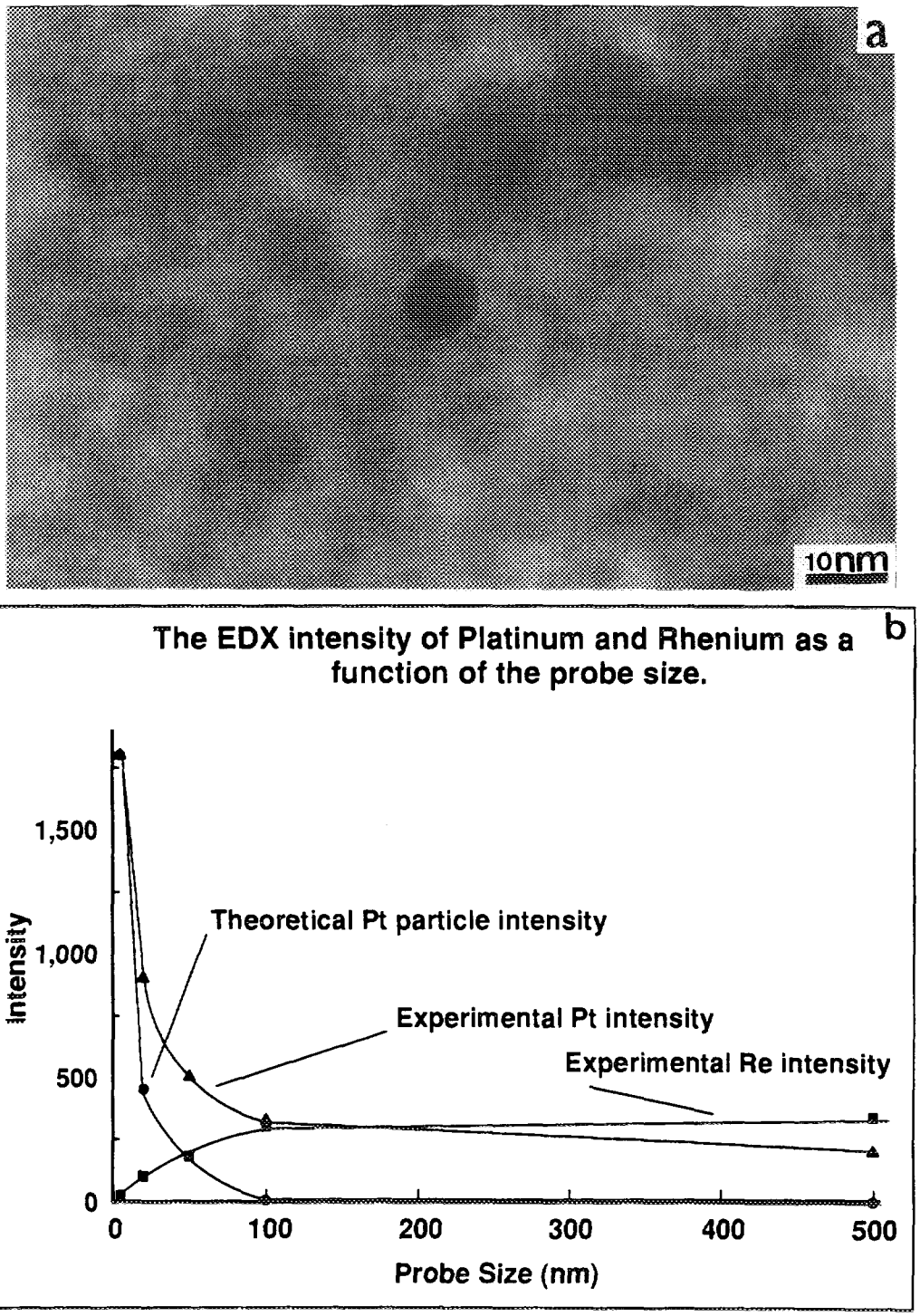

FIG. 12. EUROPT-4 after use in octane reforming: (a) TEM microgarph; (b) EDX intensity of Pt and Re as a function of the probe size.

can be associated with the platinum atoms and rhenium was not in the metallic state in the reduced EUROPT-4. (ii) CO was associated with both platinum and rhenium. The TEM and EDX results have indicated that there was no alloy formation between platinum and rhenium in the bimetallic catalysts and that rhenium in the large particles was in the ionic state. It is unlikely that rhenium existed in the metallic state in small particles, since both metallic

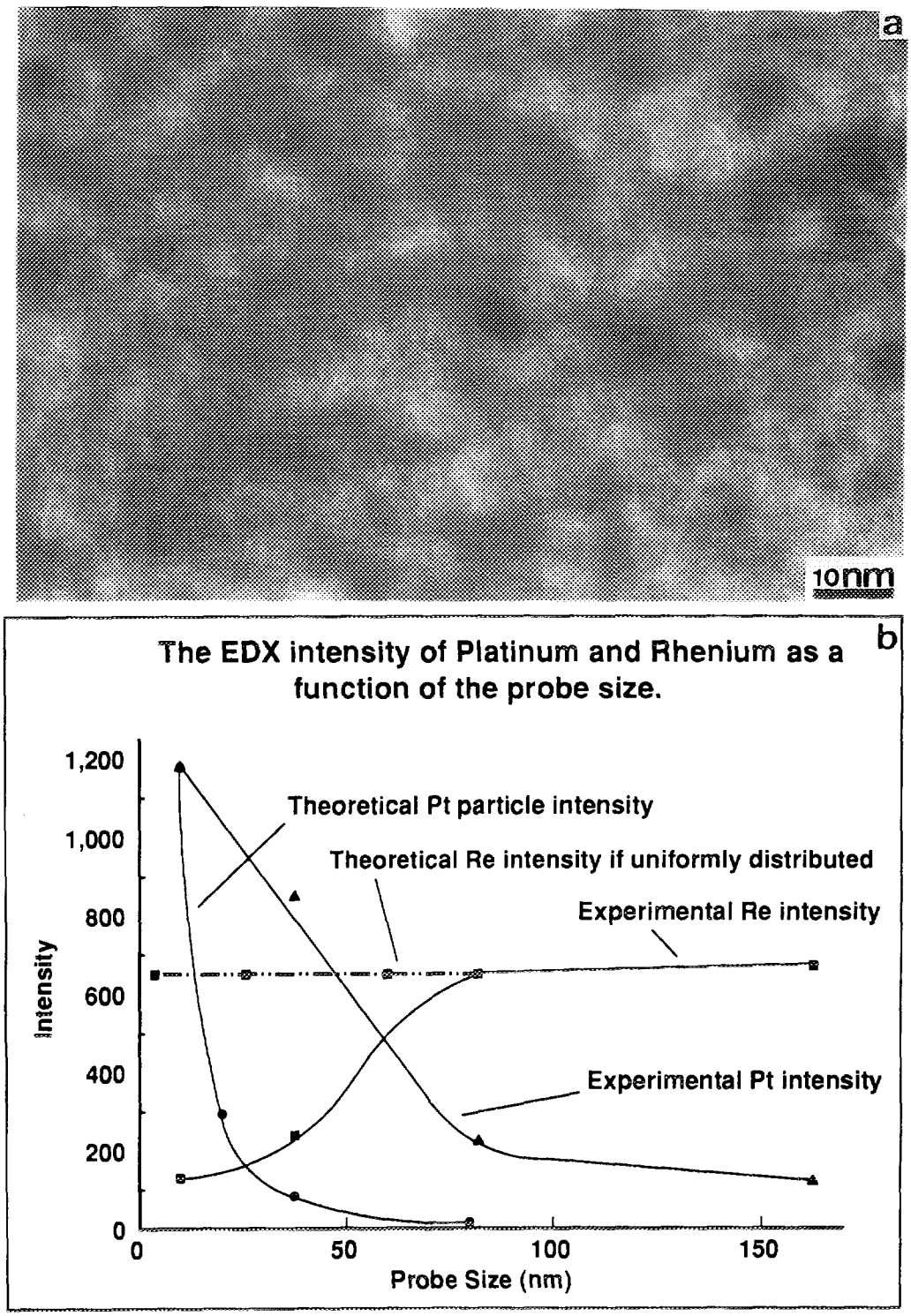

FIG. 13. 3.0 wt.% Pt–3.0 wt.% Re/γ-Al_2O_3 catalysts after use in octane reforming: (a) TEM micrograph; (b) EDX intensity of Pt and Re as a function of the probe size.

rhenium and platinum would act as nuclei to catalyse the reduction of rhenium oxide (9–11, 21), resulting in the formation of metallic rhenium in the large particles. The TEM results have also indicated that platinum was well dispersed in the EUROPT-4. If there was a significant amount of metallic rhenium, the amount of chemisorbed

TABLE 2

CO Chemisorption Results for Pt/γ-Al_2O_3, Re/γ-Al_2O_3, and Pt–Re/γ-Al_2O_3 Catalysts

Specimens	Reduction temp. (K)	CO Adsorbed (μmol)	CO_{ad}/Pt
EUROPT-3 (0.5 g)	673	0.46	0.64
EUROPT-4 (0.5 g)	673	0.45	0.63
3 wt.% Pt (0.1 g)	673	0.53	0.37
3 wt.% Re (0.5 g)	673	0	
3 wt.% Re (0.5 g)	953	0	
3 wt.% Pt–3 wt.% Re (0.2 g)	673	0.44	0.14
3 wt.% Pt–3 wt.% Re (0.2 g)	953	0.25	0.08

CO would be expected to be much higher for EUROPT-4 than EUROPT-3, and this was not found to be the case. Therefore the results can best be explained by assuming that all the adsorbed CO was associated with platinum and that rhenium was in the nonmetallic state. As discussed before, the possibility that a few percent of rhenium was reduced to the metallic state could not be ruled out.

The amount of CO adsorbed for the 3.0 wt.% Pt–3.0 wt.% Re/γ-Al_2O_3 catalyst reduced at 953 K was less than that for the same catalyst reduced at 673 K, indicating that some platinum sintering occurred in the catalyst during the reduction at the high temperature of 953 K.

Our results appear to suggest that the increased stability and selectivity to cycloalkanes and aromatics induced by the addition of rhenium to the Pt/γ-Al_2O_3 reforming catalysts arises primarily from the interaction of the rhenium oxide with the alumina support. This modifies the catalytic bifunctional nature of the Pt/γ-Al_2O_3. The modification of the support increases the selectivity of the catalyst for isomerisation with a reduction in the extent of cracking. The modification of the support also makes the catalysts more stable, and the platinum surface less susceptible to poisoning. It is impossible to say whether all the platinum particles would be affected by this modification of the support, although, intuitively, we would expect the highly dispersed smaller particles (<1 nm) that are in intimate contact with the support to be most affected. There may be some indirect interactions between the small platinum particles and the rhenium oxide phase but such interactions do not necessarily imply alloy formation.

CONCLUSIONS

(1) Two types of platinum have been identified in Pt/γ-Al_2O_3 and Pt–Re/γ-Al_2O_3 catalysts: (i) platinum particles of ~2–10 nm and (ii) very small platinum particles (<1 nm).

(2) On the evidence of this study, the majority of the Re was evenly distributed on the surface of the alumina but decreased in the vicinity of the Pt particles in the Pt–Re/γ-Al_2O_3 catalyst. The majority of rhenium was present as ReO_2 in the catalyst containing both Pt and Re, even after full reduction. The rhenium oxide modified the alumina surface.

(3) No Pt–Re alloy or bimetallic cluster was observed in the catalyst containing both Pt and Re. The possibility that a few percent of rhenium was dissolved in the platinum particle was not ruled out.

(4) Platinum aggregation occurred during the reforming reaction.

ACKNOWLEDGMENTS

Financial support from SERC and the Initiative in Interfaces and Catalysis are gratefully acknowledged. Z. H. thanks Mr. D. Thom for technical help.

REFERENCES

1. Beltramini, J., and Trimm, D. L., *Appl. Catal.* **32,** 71 (1987).
2. Charcosset, H., Fréty, R., Leclercq, G., Mendes, E., Primet, M., and Tournayan, L., *J. Catal.* **56,** 468 (1979).
3. Shpiro, E. S., Avaev, V. I., Antoshin, G., Ryashentseva, M. A., and Minachev, Kh. M., *J. Catal.* **55,** 402 (1978).
4. Schay, Z., Matusek, K., and Guczi, L., *Appl. Catal.* **10,** 173 (1984).
5. Kelley, M. J., Freed, R. L., and Swartzfager, D. G., *J. Catal.* **78,** 445 (1982).
6. Isaacs, B. H., and Petersen, E. E, *J. Catal.* **85,** 1 (1984).
7. Isaacs, B. H, and Petersen, E. E., *J. Catal.* **85,** 8 (1984).
8. Isaacs, B. H, and Petersen, E. E, *J. Catal.* **77,** 43 (1982).
9. Wagstaff, N., and Prins, R., *J. Catal.* **59,** 434 (1979).
10. Bolivar, C., Charcosset, H., Fréty, R., Primet, M., Tournayan, L., Betizeau, C., Leclercq, G., and Maurel, R., *J. Catal.* **39,** 249 (1975).
11. Bolivar, C., Charcosset, H., Fréty, R., Primet, M., Tournayan, L., Betizeau, C., Leclercq, G., and Maurel, R., *J.Catal.* **45,** 163 (1976).

12. Augustine, S. M., and Sachtler, W. M. H., *J. Catal.* **106,** 417 (1987).
13. Nacheff, M. S., Kraus, L. S., Ichikawa, M., Hoffman, B. M., Butt, J. B., Sachtler, W. M. H., *J. Catal.* **106,** 263 (1987).
14. Joseens, L. W., and Petersen, E. E, *J. Catal.* **76,** 265 (1982).
15. Biloen, P., Helle, J. N., Verbeek, H., Dautzenberg, F. M., and Sachtler, W. M. H., *J. Catal.* **63,** 112 (1980).
16. Johnson, M. F. L., and LeRoy, V. M., *J. Catal.* **35,** 434 (1974).
17. Short, D. R., Khalid, S. M., Katzer, J. R., and Kelley, M. J., *J. Catal.* **72,** 288 (1981).
18. Peri, J. B., *J. Catal.* **52,** 144 (1978).
19. McNicol, B. D., *J. Catal.* **46,** 438 (1977).
20. Johnson, M. F. L., *J. Catal.* **39,** 487 (1975).
21. Mieville, R. L., *J. Catal.* **87,** 437 (1984).
22. Bertolacini, R. J., and Pellet, R. J., *in* "Catalyst Deactivation" (B. Delmon and G. F. Froment, Eds.), p. 73. Elsevier, Amsterdam, 1980.
23. Gai-Boyes, P. L., *Catal. Rev.—Sci. Eng.* **34,** 1 (1992).
24. Yacaman, M. J., and Avalos-borja, M., *Catal. Rev.—Sci. Eng.* **34,** 55 (1992).
25. Datye, A. K., and Smith, D. J., *Catal. Rev.—Sci. Eng.* **34,** 129 (1992).
26. Park, C., and Webb, G., to be published.
27. Jackson, S. D., Glanville, B. M., Willis, J., McLellan, G. D., Webb, G., Moyes, R. B., Simpson, S., Wells, P. B., and Whyman, R., *J. Catal.* **139,** 207 (1993).
28. Goldstein, J. J., *in* "Introduction to Analytical Electron Microscopy" (J. I. Hren, J. I. Goldstein, and D. C. Joy, Eds.), p. 83. New York, 1979.
29. Flynn, P. C., Wanke, S. E., and Turner, P. S., *J. Catal,.* **33,** 233 (1974).
30. Yacaman, M. J., and Dominguez, J. M., *J. Catal.* **67,** 475 (1981).
31. Freel, J., *Prepr.—Am. Chem. Soc., Div. Pet. Chem.* **18,** 10 (1973).
32. Yao, H. C., and Shelef, M., *J. Catal.* **44,** 392 (1976).
33. Butterly, L. J., Baird, T., Fryer, J. R., Day, M., and Norval, S., *in* "Proceedings, XIth International Congress on Electron Microscopy" (T. Imura, S. Maruse, and T. Suzuki, Eds.), Vol. II, p. 1775. The Japanese Society of Electron Microscopy, Tokyo, 1986.
34. Burch, R., *J. Catal.* **71,** 348 (1981).
35. Burch, R., and Garla, L. C., *J. Catal.* **71,** 360 (1981).
36. Bond, G. C., "Catalysis by Metals." Academic Press, London, 1962.
37. Kelly, D. G., Gellman, A. J., Salmeron, M., Somorjai, G. A., Maurice, V., Huber, M., and Oudar, J., *Surf. Sci.* **204,** 1 (1988).
38. Herz, R. K., and McCready, D. F., *J. Catal,.* **81,** 358 (1983).
39. Dorling, T. A., and Moss, R. L., *J. Catal.* **7,** 378 (1967).
40. Roy, J. M., Ph.D thesis, University of Glasgow, 1992.